nature genetics

UV-sensitive syndrome protein UVSSA recruits USP7 to regulate transcription-coupled repair

Petra Schwertman[1], Anna Lagarou[2], Dick H W Dekkers[3], Anja Raams[1], Adriana C van der Hoek[1], Charlie Laffeber[1], Jan H J Hoeijmakers[1], Jeroen A A Demmers[3], Maria Fousteri[2], Wim Vermeulen[1] & Jurgen A Marteijn[1]

Transcription-coupled nucleotide-excision repair (TC-NER) is a subpathway of NER that efficiently removes the highly toxic RNA polymerase II blocking lesions in DNA. Defective TC-NER gives rise to the human disorders Cockayne syndrome and UV-sensitive syndrome (UV^{S}S)[1]. NER initiating factors are known to be regulated by ubiquitination[2]. Using a SILAC-based proteomic approach, we identified UVSSA (formerly known as KIAA1530) as part of a UV-induced ubiquitinated protein complex. Knockdown of *UVSSA* resulted in TC-NER deficiency. *UVSSA* was found to be the causative gene for UV^{S}S, an unresolved NER deficiency disorder[3]. The UVSSA protein interacts with elongating RNA polymerase II, localizes specifically to UV-induced lesions, resides in chromatin-associated TC-NER complexes and is implicated in stabilizing the TC-NER master organizing protein ERCC6 (also known as CSB) by delivering the deubiquitinating enzyme USP7 to TC-NER complexes. Together, these findings indicate that UVSSA-USP7–mediated stabilization of ERCC6 represents a critical regulatory mechanism of TC-NER in restoring gene expression.

Nucleotide-excision repair removes a wide range of DNA damage, including UV-induced lesions. Inherited NER defects lead to extreme cancer proneness (xeroderma pigmentosum) or dramatic premature aging (Cockayne syndrome), showing the clinical impact of NER[4]. NER is initiated by two damage recognition pathways: global genome NER (GG-NER) and transcription-coupled NER (TC-NER). DNA helix–distorting injuries located throughout the genome are repaired by GG-NER to avoid replication-induced mutations and resultant cancer. TC-NER targets transcription-blocking lesions to enable recovery of arrested transcription, thereby preventing damage-induced apoptosis and resultant aging. In addition, it was shown that TC-NER is also important in overcoming UV-induced transcription-associated mutations[5].

NER is regulated in response to UV irradiation by ubiquitination[2] of the process-initiating factors xeroderma pigmentosum group C (XPC)[6] and DNA damage–binding protein 2 (DDB2)[7] in GG-NER and Cockayne syndrome group B (CSB, also known as ERCC6) and the largest subunit of RNA polymerase II (RNA Pol II) in TC-NER[8–10]. However, how the entire pathway is controlled via ubiquitination remains enigmatic. To characterize the UV-induced ubiquitination network, we performed an unbiased proteomic analysis of differentially ubiquitinated protein complexes after UV irradiation. Using a ubiquitin-binding (FK2) resin and selecting for mono- and polyubiquitinated proteins[11], we achieved a strong and specific enrichment of endogenously ubiquitinated protein complexes (**Supplementary Fig. 1a**). With stable isotope labeling by amino acids in cell culture (SILAC)-based proteomics, we compared UV-treated and mock-treated cells and identified 50 upregulated and 13 down-regulated proteins that were changed (by >1.5-fold) in response to UV (**Fig. 1a**). The prominent presence of four known ubiquitin-regulated NER factors, DDB2, XPC, RNA Pol II and ERCC6 (**Fig. 1a**)[6–9], at the very top of the list of enriched proteins shows the validity of our approach. The first unknown candidate was UVSSA (UV-stimulated scaffold protein A, encoded by a predicted gene *KIAA1530* (ref. 12)), which has been renamed, with support from the Human Gene Nomenclature Committee (HGNC) (**Fig. 1a**). UVSSA is a highly conserved 709 amino acid protein predicted to contain two conserved yet poorly characterized domains (**Supplementary Fig. 1b**,**c**): an N-terminal Vps27-Hrs-STAM (VHS) domain[13] and a C-terminal DUF2043 domain[14]. To verify UVSSA ubiquitination, we coexpressed HA-tagged ubiquitin (HA-Ub) and Flag-tagged UVSSA (UVSSA-Flag) in U2OS cells and identified monoubiquitinated UVSSA after both HA-Ub or Flag-UVSSA immunoprecipitation (**Supplementary Fig. 1d**,**e**). Unexpectedly, UVSSA ubiquitination did not increase in response to UV. As this screen was performed under non-denaturing conditions, it is possible that UVSSA was isolated as part of a UV-induced ubiquitinated protein complex and that it is implicated in the UV DNA damage response (DDR) independent of its own ubiquitination status. To test this possibility, we employed RNA interference to deplete *UVSSA* in NER-proficient U2OS cells (**Supplementary Fig. 2a**) and observed clear UV hypersensitivity, similar to that achieved with knockdown of known NER factors (**Fig. 1b**). In addition, *UVSSA* knockdown resulted in IlludinS hypersensitivity (**Fig. 1c**), indicative of a role of UVSSA in TC-NER but not in GG-NER, as this drug specifically sensitizes

[1]Department of Genetics and Netherlands Proteomics Centre, Centre for Biomedical Genetics, Erasmus Medical Centre, Rotterdam, The Netherlands. [2]Institute of Molecular Biology and Genetics, Biomedical Sciences Research Centre Alexander Fleming, Athens, Greece. [3]Proteomics Centre, Erasmus University Medical Centre, Rotterdam, The Netherlands. Correspondence should be addressed to W.V. (w.vermeulen@erasmusmc.nl) or J.A.M. (j.marteijn@erasmusmc.nl).

Received 26 September 2011; accepted 29 February 2012; published online 1 April 2012; doi:10.1038/ng.2230

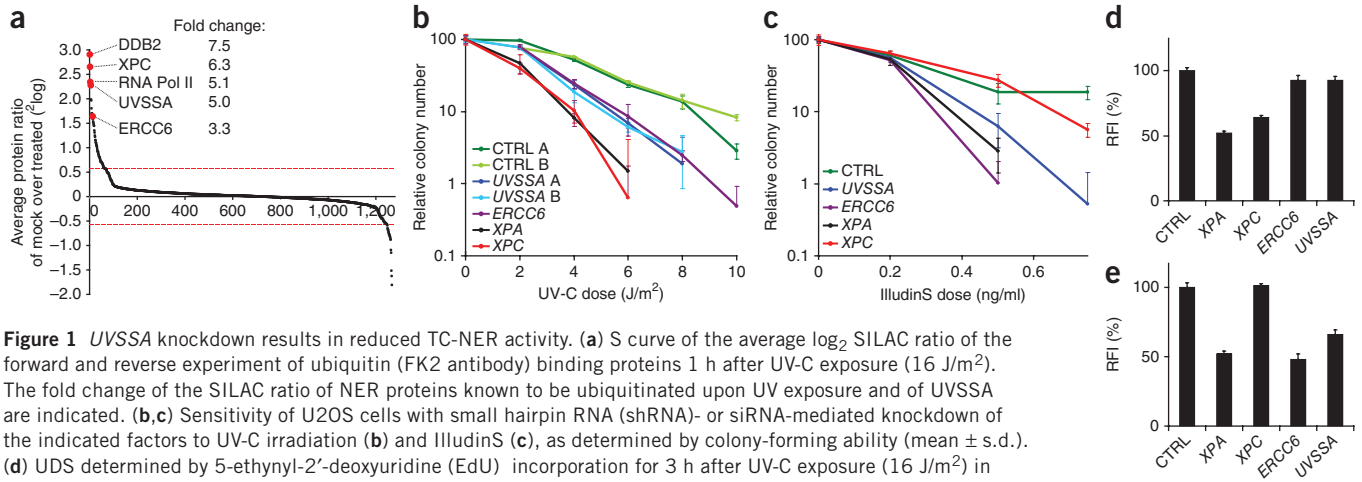

Figure 1 *UVSSA* knockdown results in reduced TC-NER activity. (**a**) S curve of the average $\log_2$ SILAC ratio of the forward and reverse experiment of ubiquitin (FK2 antibody) binding proteins 1 h after UV-C exposure (16 J/m^2). The fold change of the SILAC ratio of NER proteins known to be ubiquitinated upon UV exposure and of UVSSA are indicated. (**b**,**c**) Sensitivity of U2OS cells with small hairpin RNA (shRNA)- or siRNA-mediated knockdown of the indicated factors to UV-C irradiation (**b**) and IlludinS (**c**), as determined by colony-forming ability (mean ± s.d.). (**d**) UDS determined by 5-ethynyl-2′-deoxyuridine (EdU) incorporation for 3 h after UV-C exposure (16 J/m^2) in primary VH10 cells after siRNA-mediated knockdown of the indicated factors. (**e**) RRS after UV-induced inhibition, with 2 h of pulse labeling with 5-ethynyl uridine (EU), 16 h after UV-C exposure (12 J/m^2) in U2OS cells with siRNA-mediated knockdown of the indicated factors. In **d** and **e**, $n > 200$ cells per sample. RFI, relative fluorescence intensity (mean ± s.e.m.).

TC-NER–deficient cells[15]. The specific role of UVSSA in TC-NER was further shown, as knockdown resulted in a clear reduction of recovery of RNA synthesis (RRS) after UV irradiation, a measure that is specific for TC-NER[16], whereas no effect was found on UV-induced DNA repair synthesis (UDS), which is mainly a measure of GG-NER efficiency[16] (**Fig. 1d**,**e** and **Supplementary Fig. 2b**). Together, these data show that UVSSA is specifically implicated in TC-NER.

The specific TC-NER deficiency after *UVSSA* knockdown strongly parallels the cellular TC-NER defect of individuals with UV-sensitive syndrome (UV^{S}S)[3,17]. UV^{S}S is a rare autosomal recessive disorder characterized by photosensitivity and mild freckling but, in contrast to Cockayne syndrome, occurs without neurological abnormalities. UV^{S}S is genetically heterogeneous, which is caused by mutations in either *ERCC6*, *ERCC8* (*CSA*) or the previously unknown *UV^{S}SA* causal gene[3,17–19]. To test whether *UVSSA* was the causative gene of UV^{S}S, we expressed differently tagged UVSSA proteins (**Supplementary Fig. 2c**) in the UV^{S}S group A (UV^{S}S-A) cell line TA-24 (ref. 17). UVSSA expression restored UV and IlludinS sensitivity (**Fig. 2a**,**b**) and RRS deficiency (**Fig. 2c**,**d**) to wild-type levels. In addition, immunoblot analysis showed that the UVSSA protein was absent in UV^{S}S-A cells relative to GG-NER–deficient (XP-C) or TC-NER–deficient (CS-B) cells (**Fig. 2e**). Together with mutational analysis of *UVSSA* in accompanying papers by Zhang *et al.*[20] and Nakazawa *et al.*[21], our data show that *UVSSA* is the causative gene in UV-sensitive syndrome and also establish that the encoded protein is a new TC-NER factor.

To investigate the *in vivo* role of UVSSA, we measured the dynamic association of UVSSA with NER in living cells. Green fluorescent protein (GFP)-tagged UVSSA, which was shown to be biologically active (**Fig. 2a–d**), accumulated at local UV-C DNA damage (LUD). LUD was either induced by a 266 nm UV-C laser[22] (**Fig. 3a**,**b**) or by irradiation with a 254 nm UV-C lamp through a microporous filter[23] (**Supplementary Fig. 3a**,**b**). Recruitment kinetics of GFP-UVSSA to LUD were strikingly similar to those of the TC-NER factor ERCC6 but were markedly different from the assembly rate of the GG-NER factors DDB2 and XPC (**Fig. 3a**,**b**). Inhibition of transcription by α-amanitin substantially attenuated the association of GFP-UVSSA with LUD (**Fig. 3a**,**b**), consistent with a role of UVSSA in TC-NER. UVSSA still accumulated at LUD in XP-C, XP-A, CS-A and CS-B cells (**Fig. 3c**), indicating that UVSSA accumulates early in the TC-NER process. Our ubiquitinome analysis, performed under non-denaturing conditions, showed that UVSSA was enriched to the same extent as RNA Pol II (fivefold; **Fig. 1a**), which is known to be polyubiquitinated in response to UV[8,10]. This might suggest that UVSSA is copurified as part of an RNA Pol II–containing protein complex, such as lesion-stalled elongating RNA Pol II. To test this possibility, we compared the mobility of GFP-UVSSA by measuring fluorescence recovery after photobleaching (FRAP) in the presence of different transcription inhibitors. The DNA-intercalating drug actinomycin D, which strongly immobilizes GFP–RNA Pol II as a result of stalling at intercalating molecules[24], also resulted in immobilization of GFP-UVSSA (**Fig. 3d**), as was the case

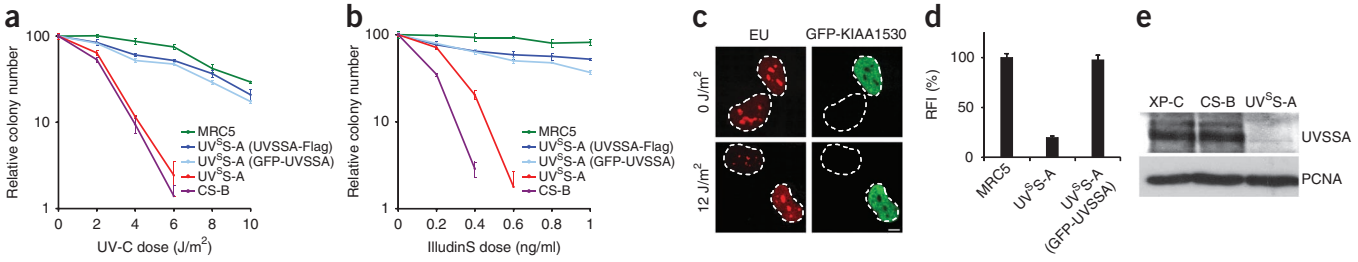

Figure 2 UVSSA expression rescues TC-NER deficiency in UV^{S}S-A (TA-24) cells. (**a**,**b**) Colony survival of NER-proficient MRC5 cells, TC-NER–deficient CS-B (CS1AN) cells and the cell lines from subjects with UV^{S}S-A TA-24 after UV-C irradiation (**b**) and IlludinS treatment (**c**). Expression of Flag- or GFP-tagged UVSSA rescues the UV-sensitive phenotype of UV^{S}S-A cells (mean ± s.d.). (**c**) *In situ* transcription in UV^{S}S-A cells with and without expression of GFP-UVSSA, before and 16 h after UV-C exposure (12 J/m^2), as measured by EU pulse labeling. Scale bar, 7 μm. (**d**) RRS activity of MRC5, UV^{S}S-A and GFP-UVSSA–expressing UV^{S}S-A cells with 2 h of pulse labeling with EU, 16 h after UV-C exposure (12 J/m^2) ($n > 200$ cells, mean ± s.e.m.). RFI, relative fluorescence intensity. (**e**) Immunoblot analysis of UVSSA in chromatin fractions of XP-C (XP4PA), CS-B (CS1AN) and UV^{S}S-A (TA-24) cells. PCNA staining was used as loading control.

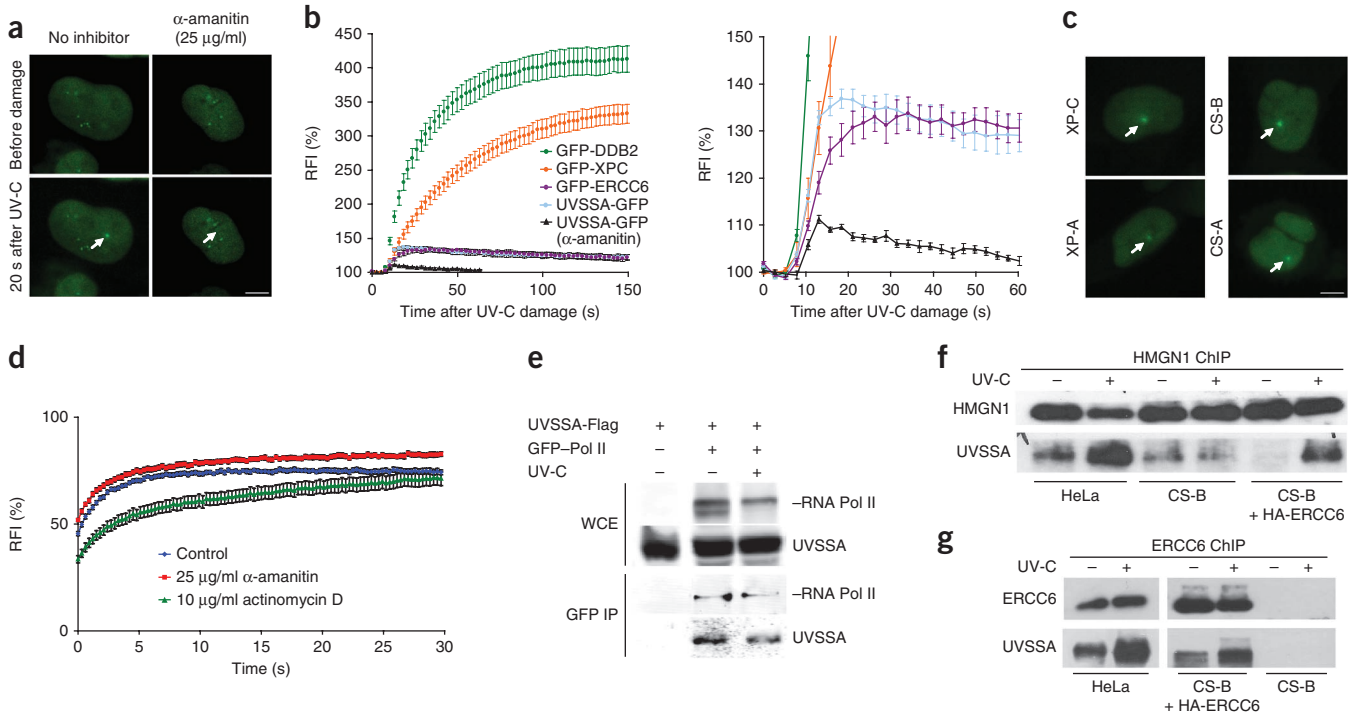

Figure 3 UVSSA is recruited to active TC-NER sites in a UV damage– and transcription-dependent manner. (**a**) LUD infliction (arrows) in MRC5 cells stably expressing UVSSA-GFP. Right, cells were pretreated with 25 μg/ml α-amanitin for 16 h. Scale bar, 7 μm. (**b**) GFP fluorescence intensity of the indicated proteins at LUD relative to pre-damage intensity were recorded over time using live-cell confocal imaging ($n > 10$ cells, mean ± s.e.m.). Right, magnification of the early time points. (**c**) XP-C (XP4PA), XP-A (XP2OS), CS-B (CS1AN) and CS-A (CS3BE) cells stably expressing GFP-tagged UVSSA were exposed to UV-C (266 nm) laser–induced damage (arrows). Scale bar, 7 μm. (**d**) Graph of FRAP results in which the relative fluorescence recovery after bleaching is plotted against the time after UVSSA-expressing MRC5 cells were untreated or treated with 25 μg/ml α-amanitin (16 h) or 10 μg/ml actinomycin D (1 h). RFI, relative fluorescence intensity. (**e**) U2OS cells cotransfected with GFP–RNA Pol II and UVSSA-Flag were subjected to GFP immunoprecipitation. Cells were UV-C irradiated (60 J/m^2) 1 h before cell lysis. WCE, whole-cell extract; IP, immunoprecipitate. (**f**,**g**) ChIP analysis of *in vivo* cross-linked HeLa, CS-B (CS1AN) or HA-ERCC6–complemented CS-B cells, which were subjected to HMGN1 (**f**) or ERCC6 (**g**) ChIP 1 h after mock or UV-C treatment (20 J/m^2). Immunoblot analysis of the coimmunoprecipitated proteins was performed with the indicated antibodies.

with GFP-ERCC6 (ref. 25). In contrast, α-amanitin released RNA Pol II from DNA, which also resulted in increased mobility of UVSSA. The opposing effects by these transcription inhibitors on GFP-UVSSA mobility in living cells cannot be caused by an indirect UVSSA interaction with RNA Pol II via ERCC6 (ref. 25), as similar effects were found in CS-B cells (**Supplementary Fig. 3c**).

Because these findings argue for an interaction of UVSSA with the protein complex containing the elongating form of RNA Pol II (RNA Pol IIo), we performed coimmunoprecipitation experiments. Indeed, UVSSA-Flag coprecipitated with GFP–RNA Pol II in U2OS cells in equal amounts before or after UV damage (**Fig. 3e**). In addition, using a specialized chromatin immunoprecipitation (ChIP) procedure aimed at revealing endogenous TC-NER interacting proteins[26], we found that chromatin-bound RNA Pol IIo also interacts with UVSSA in a UV-independent manner (**Supplementary Fig. 3d**) in UVSSA-expressing UV^{S}S-A and CS-B cells. This UV-independent UVSSA–RNA Pol II interaction explains the enrichment of UVSSA in our ubiquitin screen after UV irradiation (**Fig. 1a**), as this protein will be copurified by virtue of the enhanced ubiquitination of RNA Pol IIo in response to UV[8], thereby explaining the similar SILAC ratio for both proteins. Together, these data suggest that UVSSA dynamically interacts with active transcription complexes.

To examine whether UVSSA is also present in active, chromatin-bound TC-NER complexes via its interaction with RNA Pol IIo, we performed ChIP experiments with antibodies against HGMN1, a chromatin remodeler that is enriched in lesion-stalled TC-NER complexes[26]. This analysis revealed a clear UV-dependent interaction of endogenous UVSSA with active, chromatin-bound TC-NER complexes in TC-NER–proficient cells (**Fig. 3f**). The UVSSA-HMGN1 interaction was absent in CS-B cells, consistent with the notion that HMGN1 is not recruited to TC-NER complexes in the absence of ERCC6 (ref. 26), showing that UVSSA only resides in HMGN1 complexes that are active in TC-NER. Using antibodies to ERRC6 for ChIP, we confirmed the UV-induced enrichment of UVSSA in active TC-NER complexes upon UV damage (**Fig. 3g**). Because UVSSA is targeted to active TC-NER complexes and is essential for efficient transcription restart after UV damage[17], we tested whether UVSSA is involved in the recruitment of the TC-NER master organizer ERCC6 to sites of UV damage. Knockdown of *UVSSA* attenuated the assembly of GFP-ERCC6 on LUD (**Fig. 4a**), whereas it did not affect XPC (GG-NER) accumulation (**Supplementary Fig. 4a**). In addition, we noted that with *UVSSA* depletion in cells stably expressing GFP-ERCC6 (ref. 25), the total level of GFP-ERCC6 fluorescence was decreased (**Supplementary Fig. 4b**). ERCC6 protein levels are controlled by the ubiquitin-proteasome system after UV damage[9]. To test whether UVSSA has an effect on ERCC6 stability, we quantified endogenous ERCC6 levels in UV^{S}S-A and GFP-UVSSA–complemented UV^{S}S-A cells at different time points after UV irradiation (**Fig. 4b** and **Supplementary Fig. 4c**). In UV^{S}S-A cells, we observed a clear proteasome- and UV-dependent decrease in ERCC6 levels compared to UVSSA-complemented UV^{S}S-A cells. The levels of RNA Pol II were equally reduced in both cell lines[8]; however, RNA Pol II reappeared 8 h after UV damage only in the complemented UV^{S}S-A cells.

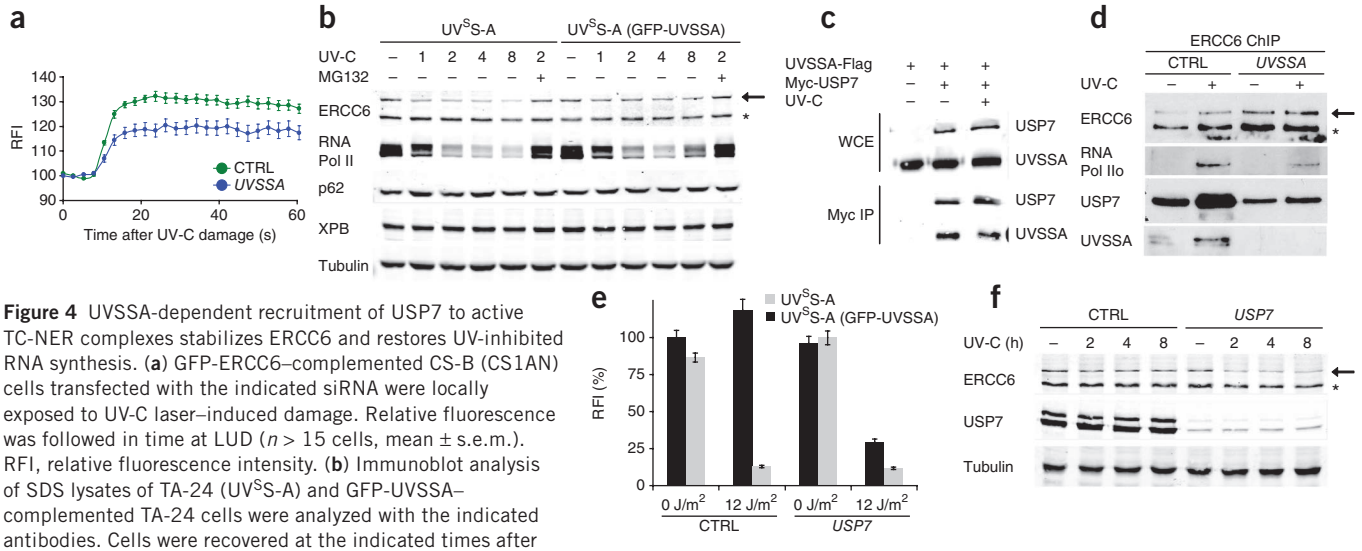

Figure 4 UVSSA-dependent recruitment of USP7 to active TC-NER complexes stabilizes ERCC6 and restores UV-inhibited RNA synthesis. (**a**) GFP-ERCC6–complemented CS-B (CS1AN) cells transfected with the indicated siRNA were locally exposed to UV-C laser–induced damage. Relative fluorescence was followed in time at LUD ($n > 15$ cells, mean ± s.e.m.). RFI, relative fluorescence intensity. (**b**) Immunoblot analysis of SDS lysates of TA-24 (UV^{S}S-A) and GFP-UVSSA–complemented TA-24 cells were analyzed with the indicated antibodies. Cells were recovered at the indicated times after UV-C exposure (12 J/m^2). MG132 (50 μM) was added at the time of UV-C exposure. ERCC6 levels (arrow) were quantified relative to those of the ERCC6-PiggyBac fusion protein[36] (asterisk) (**Supplementary Fig. 4c**). (**c**) U2OS cells cotransfected with Myc-USP7 and UVSSA-Flag were subjected to Myc immunoprecipitation. Cells were UV-C irradiated (20 J/m^2) 1 h before cell lysis. WCE, whole-cell extract, IP, immunoprecipitate. (**d**) U2OS cells stably expressing the indicated shRNA were subjected to ERCC6-specific ChIP followed by immunoblotting for the indicated proteins. (**e**) RRS activity of TA-24 (UV^{S}S-A) and GFP-UVSSA–complemented TA-24 cells transfected with the indicated siRNA before and 16 h after UV-C irradiation (12 J/m^2) ($n > 200$ cells, mean ± s.e.m.). RFI, relative fluorescence intensity. (**f**) U2OS cells were transfected with control or *USP7* siRNA, harvested at the indicated time points after UV-C exposure (12 J/m^2) and stained for ERCC6, USP7 and tubulin. ERCC6 levels (arrow) were quantified relative to those of the ERCC6-PiggyBac fusion protein[36] (asterisk) (**Supplementary Fig. 6b**).

Whether this RNA Pol II recovery is a direct effect of UVSSA or an indirect consequence of rescued TC-NER remains to be determined.

In order to examine how UVSSA influences ERCC6 protein stability, we immunoprecipitated GFP-UVSSA and analyzed UVSSA-interacting proteins by mass spectrometry. Of note, we identified the deubiquitinating enzyme ubiquitin carboxyl-terminal hydrolase 7 (USP7, also called HAUSP) that is known to have various functions in DDR[27–30], as one of the most prominent interacting partners of UVSSA (**Supplementary Fig. 4d**). This interaction was confirmed by coimmunoprecipitation of UVSSA-Flag with Myc-USP7 (**Fig. 4c**). Moreover, we showed that endogenous USP7 resides in chromatin immunoprecipitated TC-NER complexes in a UV- and UVSSA-dependent manner (**Fig. 4d** and **Supplementary Fig. 5a**,**b**). Like the UVSSA–RNA Pol II interaction, the UVSSA-mediated USP7–RNA Pol II interaction is not increased after UV damage (**Supplementary Fig. 5c**). This suggests that USP7 is recruited to TC-NER complexes via its interaction with UVSSA. As UVSSA is missing in UV^{S}S-A cells, decreased ERCC6 stability after UV could be explained by the absence of USP7 deubiquitinating activity in the TC-NER complex. Indeed, depletion of *USP7* by RNA interference (**Supplementary Fig. 6a**) caused a similar defect in RRS (**Fig. 4e**) and in reduction of ERCC6 levels (**Fig. 4f** and **Supplementary Fig. 6b**–**d**) after UV irradiation as UVSSA deficiency. These data suggest that USP7, recruited by UVSSA, has an important role in TC-NER. Additionally, the absence of further sensitization to the RRS defect by combined interference with *UVSSA* and *USP7* expression (**Fig. 4e**) suggests that these genes are epistatic.

In summary, within our mass spectrometry analysis of the UV-induced ubiquitinome, we identified an uncharacterized protein (UVSSA), which was highly enriched upon UV irradiation in immunopurified ubiquitinated protein complexes. Functional analysis indicated that UVSSA is a new factor implicated in TC-NER and, of note, is the causative gene in the unresolved UV^{S}S-A NER disorder. Two accompanying studies aimed at finding the genetic defect in UV^{S}S-A also identified *UVSSA* as the gene mutated in individuals with UV^{S}S-A[20,21]. Their further functional analysis is consistent with our observation that UVSSA has an important role in TC-NER and is part of the protein complex containing the elongating form of RNA Pol II. Our data argue for a UV-independent UVSSA–RNA Pol IIo interaction. In contrast to GFP-UVSSA, we were not able to observe RNA Pol IIo accumulation at LUD with current technology. The transient or low-affinity interaction between UVSSA and RNA Pol IIo might be stabilized upon UV irradiation, explaining the UV dependency observed in native immunoprecipitations[20] and the UV independence of the fixed interactions by cross-linking in ChIP shown here.

We propose a model (**Supplementary Fig. 6f**) in which one of the key functions of UVSSA in TC-NER is to protect ERCC6 against UV-induced degradation, by targeting the deubiquitinating enzyme USP7 to lesion-stalled RNA Pol II complexes. Of note, overexpression of ERCC6 in UV^{S}S-A cells did not correct the TC-NER defect (**Supplementary Fig. 6e**), suggesting that the reduced levels of ERCC6 observed in UV^{S}S-A cells is not sufficient to explain the UV^{S}S phenotype. This suggests that deubiquitination of ERCC6 by UVSSA is an essential step for proper TC-NER, either to provide an increased time frame for this key assembly factor to orchestrate TC-NER complex formation or to inhibit a ubiquitin-mediated functional change in ERCC6. In cells with *UVSSA* knockdown, reduced interaction was observed between RNA Pol IIo and ERCC6 (**Fig. 4d**). Whether this reduced interaction is a direct consequence or is independent of ERCC6 ubiquitination remains to be elucidated. Either way, our data show the importance of the delicate ERCC6 ubiquitination equilibrium during TC-NER by counteracting TC-NER–specific E3 ligases[9,31]. USP7 has multiple roles in the DNA damage response[27–30], and its pleiotropic activity is even broader, targeting tumor suppressors, immune responders, viral proteins and epigenetic modulators[32]. An important role for UVSSA might be to deliver the deubiquitinating USP7 enzyme to TC-NER, thereby providing substrate specificity to this pleiotropic deubiquitinase. The implication of UVSSA in ubiquitination of the elongating form of RNA

Pol II after UV damage[21] seems to imply that UVSSA has functions in TC-NER beyond being a specific shuttle protein for USP7.

The causative genes for the two TC-NER defective disorders Cockayne syndrome and UV^{S}S (ERCC6, ERCC8 and UVSSA) are all cofactors of lesion-stalled RNA Pol II. However, the phenotypes of these two TC-NER deficiencies are strikingly different; Cockayne syndrome is characterized by severe neurological and developmental abnormalities in conjunction with UV sensitivity, whereas individuals with UV^{S}S mainly exhibit sun sensitivity, without any clear additional complications[1]. It has been proposed that this phenotypic difference is caused by the distinct abilities of affected individuals to process certain oxidative lesions: Cockayne syndrome cells are sensitive for oxidative base damage, whereas UV^{S}S cells are not[1,19,33–35]. This suggests that UVSSA and the subsequent deubiquitination of ERCC6 by USP7 are crucial for the execution of the complete NER process, but these seem to not be essential in processing oxidative damage in transcribed strands. Of course, the possibility is not excluded that additional functions of the Cockayne syndrome proteins also contribute to the severe Cockayne syndrome phenotype. The discovery of two new TC-NER factors, UVSSA and USP7, which are both implicated in regulating TC-NER activity, represents an important advance toward further elucidation of the transcription-coupled repair process.

METHODS

Methods and any associated references are available in the online version of the paper at http://www.nature.com/naturegenetics/.

Note: Supplementary information is available on the Nature Genetics website.

ACKNOWLEDGMENTS

We thank R. Bernards and M. Epping (Nederlands Kanker Instituut) for the Myc-tagged USP7 expression construct and P. Verrijzer and A. Reddy (Erasmus Medical Centre) for sh*USP7*-expressing lentivirus. We thank H. Slor (Tel Aviv University) for the TA-24sv40 cell line and N.G.J. Jaspers and H. Lans for discussions and critical reading of the manuscript. This work was funded by the Netherlands Genomics Initiative NPCII (to P.S.), 935.19.021 and 935.11.042 (to W.V., C.L. and J.A.M.), the Dutch Organization for Scientific Research ZonMW Veni Grant (917.96.120 to J.A.M.) and TOP grant (912.08.031 to W.V.), Marie Curie FP7-PIEF-GA-2009-253544 (to M.F.), the Association for International Cancer Research (10-594 to W.V.) and the Cancer Genomics Centre and ERC (advanced research grant to J.H.J.H.).

AUTHOR CONTRIBUTIONS

D.H.W.D. and J.A.A.D. performed the mass spectrometry analyses, A.R. performed UDS and RRS experiments, A.C.v.d.H. performed immunoprecipitation experiments, C.L. provided technical assistance, and M.F. designed and, together with A.L., performed ChIP experiments. J.H.J.H. provided support and advice, and helped write the manuscript. P.S. and J.A.M. performed experiments and generated reagents. W.V. and J.A.M. designed the study and supervised the project. W.V., J.A.M. and P.S. wrote the manuscript. All authors discussed the results and commented on the manuscript.

COMPETING FINANCIAL INTERESTS

The authors declare no competing financial interests.

Published online at http://www.nature.com/naturegenetics/.
Reprints and permissions information is available online at http://www.nature.com/reprints/index.html.

1. Hanawalt, P.C. & Spivak, G. Transcription-coupled DNA repair: two decades of progress and surprises. *Nat. Rev. Mol. Cell Biol.* **9**, 958–970 (2008).
2. Bergink, S., Jaspers, N.G. & Vermeulen, W. Regulation of UV-induced DNA damage response by ubiquitylation. *DNA Repair (Amst.)* **6**, 1231–1242 (2007).
3. Itoh, T., Ono, T. & Yamaizumi, M. A new UV-sensitive syndrome not belonging to any complementation groups of xeroderma pigmentosum or Cockayne syndrome: siblings showing biochemical characteristics of Cockayne syndrome without typical clinical manifestations. *Mutat. Res.* **314**, 233–248 (1994).
4. Hoeijmakers, J.H. DNA damage, aging, and cancer. *N. Engl. J. Med.* **361**, 1475–1485 (2009).
5. Hendriks, G. *et al.* Transcription-dependent cytosine deamination is a novel mechanism in ultraviolet light–induced mutagenesis. *Curr. Biol.* **20**, 170–175 (2010).
6. Sugasawa, K. *et al.* UV-induced ubiquitylation of XPC protein mediated by UV-DDB–ubiquitin ligase complex. *Cell* **121**, 387–400 (2005).
7. Rapić-Otrin, V., McLenigan, M.P., Bisi, D.C., Gonzalez, M. & Levine, A.S. Sequential binding of UV DNA damage binding factor and degradation of the p48 subunit as early events after UV irradiation. *Nucleic Acids Res.* **30**, 2588–2598 (2002).
8. Bregman, D.B. *et al.* UV-induced ubiquitination of RNA polymerase II: a novel modification deficient in Cockayne syndrome cells. *Proc. Natl. Acad. Sci. USA* **93**, 11586–11590 (1996).
9. Groisman, R. *et al.* CSA-dependent degradation of CSB by the ubiquitin-proteasome pathway establishes a link between complementation factors of the Cockayne syndrome. *Genes Dev.* **20**, 1429–1434 (2006).
10. Anindya, R., Aygun, O. & Svejstrup, J.Q. Damage-induced ubiquitylation of human RNA polymerase II by the ubiquitin ligase Nedd4, but not Cockayne syndrome proteins or BRCA1. *Mol. Cell* **28**, 386–397 (2007).
11. Fujimuro, M., Sawada, H. & Yokosawa, H. Production and characterization of monoclonal antibodies specific to multi-ubiquitin chains of polyubiquitinated proteins. *FEBS Lett.* **349**, 173–180 (1994).
12. Nagase, T., Kikuno, R., Ishikawa, K., Hirosawa, M. & Ohara, O. Prediction of the coding sequences of unidentified human genes. XVII. The complete sequences of 100 new cDNA clones from brain which code for large proteins *in vitro*. *DNA Res.* **7**, 143–150 (2000).
13. Mizuno, E., Kawahata, K., Kato, M., Kitamura, N. & Komada, M. STAM proteins bind ubiquitinated proteins on the early endosome via the VHS domain and ubiquitin-interacting motif. *Mol. Biol. Cell* **14**, 3675–3689 (2003).
14. Bateman, A., Coggill, P. & Finn, R.D. DUFs: families in search of function. *Acta Crystallogr. Sect. F Struct. Biol. Cryst. Commun.* **66**, 1148–1152 (2010).
15. Jaspers, N.G. *et al.* Anti-tumour compounds illudin S and Irofulven induce DNA lesions ignored by global repair and exclusively processed by transcription- and replication-coupled repair pathways. *DNA Repair (Amst.)* **1**, 1027–1038 (2002).
16. Nakazawa, Y., Yamashita, S., Lehmann, A.R. & Ogi, T. A semi-automated non-radioactive system for measuring recovery of RNA synthesis and unscheduled DNA synthesis using ethynyluracil derivatives. *DNA Repair (Amst.)* **9**, 506–516 (2010).
17. Spivak, G. UV-sensitive syndrome. *Mutat. Res.* **577**, 162–169 (2005).
18. Horibata, K. *et al.* Complete absence of Cockayne syndrome group B gene product gives rise to UV-sensitive syndrome but not Cockayne syndrome. *Proc. Natl. Acad. Sci. USA* **101**, 15410–15415 (2004).
19. Nardo, T. *et al.* A UV-sensitive syndrome patient with a specific *CSA* mutation reveals separable roles for CSA in response to UV and oxidative DNA damage. *Proc. Natl. Acad. Sci. USA* **106**, 6209–6214 (2009).
20. Zhang, X. *et al.* Mutations in *UVSSA* cause UV-sensitive syndrome and destabilize ERCC6 in transcription-coupled DNA repair. *Nat. Genet.* published online (1 April 2012); doi:10.1038ng.2228.
21. Nakazawa, Y. *et al.* Mutations in *UVSSA* cause UV-sensitive syndrome and impair RNA polymerase IIo processing in transcription-coupled nucleotide-excision repair. *Nat. Genet.* published online (1 April 2012); doi:10.1038ng.2229.
22. Dinant, C. *et al.* Activation of multiple DNA repair pathways by sub-nuclear damage induction methods. *J. Cell Sci.* **120**, 2731–2740 (2007).
23. Volker, M. *et al.* Sequential assembly of the nucleotide excision repair factors *in vivo*. *Mol. Cell* **8**, 213–224 (2001).
24. Kimura, H., Sugaya, K. & Cook, P.R. The transcription cycle of RNA polymerase II in living cells. *J. Cell Biol.* **159**, 777–782 (2002).
25. van den Boom, V. *et al.* DNA damage stabilizes interaction of CSB with the transcription elongation machinery. *J. Cell Biol.* **166**, 27–36 (2004).
26. Fousteri, M., Vermeulen, W., van Zeeland, A.A. & Mullenders, L.H. Cockayne syndrome A and B proteins differentially regulate recruitment of chromatin remodeling and repair factors to stalled RNA polymerase II *in vivo*. *Mol. Cell* **23**, 471–482 (2006).
27. Faustrup, H., Bekker-Jensen, S., Bartek, J., Lukas, J. & Mailand, N. USP7 counteracts $SCF^{\beta TrCP}$- but not APC^{Cdh1}-mediated proteolysis of Claspin. *J. Cell Biol.* **184**, 13–19 (2009).
28. Khoronenkova, S.V., Dianova, I.I., Parsons, J.L. & Dianov, G.L. USP7/HAUSP stimulates repair of oxidative DNA lesions. *Nucleic Acids Res.* **39**, 2604–2609 (2011).
29. Li, M. *et al.* Deubiquitination of p53 by HAUSP is an important pathway for p53 stabilization. *Nature* **416**, 648–653 (2002).
30. Meulmeester, E. *et al.* Loss of HAUSP-mediated deubiquitination contributes to DNA damage-induced destabilization of Hdmx and Hdm2. *Mol. Cell* **18**, 565–576 (2005).
31. Wei, L. *et al.* BRCA1 contributes to transcription-coupled repair of DNA damage through polyubiquitination and degradation of Cockayne syndrome B protein. *Cancer Sci.* **102**, 1840–1847 (2011).
32. Nicholson, B. & Suresh Kumar, K.G. The multifaceted roles of USP7: new therapeutic opportunities. *Cell Biochem. Biophys.* **60**, 61–68 (2011).
33. Spivak, G. & Hanawalt, P.C. Host cell reactivation of plasmids containing oxidative DNA lesions is defective in Cockayne syndrome but normal in UV-sensitive syndrome fibroblasts. *DNA Repair (Amst.)* **5**, 13–22 (2006).
34. D'Errico, M. *et al.* The role of CSA in the response to oxidative DNA damage in human cells. *Oncogene* **26**, 4336–4343 (2007).
35. Gorgels, T.G. *et al.* Retinal degeneration and ionizing radiation hypersensitivity in a mouse model for Cockayne syndrome. *Mol. Cell. Biol.* **27**, 1433–1441 (2007).
36. Newman, J.C., Bailey, A.D., Fan, H.Y., Pavelitz, T. & Weiner, A.M. An abundant evolutionarily conserved CSB-PiggyBac fusion protein expressed in Cockayne syndrome. *PLoS Genet.* **4**, e1000031 (2008).

ONLINE METHODS

Cell lines and culture. For SILAC labeling, HeLa cells were cultured for 2 weeks in DMEM without lysine, arginine or leucine (AthenaES) supplemented with antibiotics, 10% dialyzed FCS (Invitrogen) and 105 μg/ml leucine (Sigma) and either 73 μg/ml light [$^{12}C_6$]-lysine and 42 μg/ml [$^{12}C_6$,$^{14}N_4$]-arginine (Sigma) or with heavy [$^{13}C_6$]-lysine and [$^{13}C_6$,$^{15}N_4$]-arginine (Cambridge Isotope Laboratories) at 37 °C and 5% CO_2.

U2OS, VH10 and the SV40-immortalized MRC5, TA-24 (UVSS-A), XP2OS (XP-A), XP4PA (XP-C), XP4PA (expressing GFP-XPC), CS3BE (CS-A), CS1AN (CS-B) and CS1AN (expressing GFP-ERCC6) cells were cultured in a 1:1 ratio of DMEM and Ham's F10 (Invitrogen) containing 10% FCS and antibiotics at 37 °C and 5% CO_2. Medium was supplemented with hygromycin (25 μg/ml) for MRC5 (expressing UVSSA-GFP), TA-24 (expressing GFP-UVSSA) and TA-24 (expressing UVSSA-Flag) cells.

Cells were treated with 25 mg/ml α-amanitin (16 h), 10 mg/ml actinomycin D (1 h) or 50 mM MG132. DNA damage was inflicted by 24-h exposure to IlludinS[15] or by UV-C irradiation (254 nm; TUV Lamp, Phillips).

Plasmid constructs. *UVSSA* cDNA was PCR amplified from a cDNA clone (BC110331) using the primers listed in **Supplementary Table 1**. The PCR product was cloned into pCR-Blunt-II-TOPO (Invitrogen) and transferred into pENTR1A-GFP-N2 (Addgene, plasmid 19364) and pENTR1A-GFP-C1 (Addgene, plasmid 17396) using EcoRI-SacII sites or into pENTR4 (Addgene, plasmid 17424) using EcoRI-NotI sites[37]. Recombination into the pLenti CMV Hygro destination vector (Addgene, plasmid 17454)[37] was performed with the Gateway LR Clonase II Enzyme Mix (Invitrogen).

The GFP–RNA Pol II and Myc-USP7 constructs have been previously described[38,39]. DNA transfections were performed using Lipofectamine 2000 (Invitrogen) according to the manufacturer's instructions. Third-generation lentiviruses were made in HEK293T cells.

RNA interference. Sequences for siRNA oligonucleotides (Thermo Fisher Scientific) are shown in **Supplementary Table 2**. siRNA transfections were performed using RNAiMax (Invitrogen) or Hiperfect (Qiagen), according to the manufacturer's instructions. shRNAs from the MISSION shRNA library (Sigma) were used to make third-generation lentiviruses. Target sequences are provided in **Supplementary Table 2**.

Quantitative RT-PCR. Total RNA was isolated from siRNA-transfected or shRNA-transduced U2OS cells using the RNeasy mini kit (Qiagen). cDNA was synthesized using random hexamer primers and SuperScript II Reverse Transcriptase (Invitrogen).

UVSSA and *GAPDH* expression levels were analyzed using qRT-PCR with the TaqMan Gene Expression Assay, using a Bio-Rad CFX96 device. *UVSSA* expression levels were normalized to *GAPDH* expression.

Antibodies. For immunoprecipitation, we used mouse monoclonal antibodies to monoubiquitinated and polyubiquitinated conjugates (FK2, BML-PW8810, Biomol) and Myc (9E10, sc-40, Santa Cruz Biotechnology) and FLAG-M2 antibody conjugated to agarose beads (Sigma), HA antibody conjugated to agarose beads (Sigma) and GFP antibody conjugated to agarose beads (ChromoTek). For ChIP, we used mouse monoclonal antibody to RNA Pol II (H5, Babco) and rabbit polyclonal antibodies to HMGN1 (Ab5212, Abcam) and ERCC6 (H-300, sc-25370, Santa Cruz Biotechnology). For protein blots, we used monoclonal antibodies to GFP (Roche and Santa Cruz Biotechnology), CPD (TDM-2, MBL International), HA (3F10, Roche), RNA Pol II (8wG16, Ab5095, Abcam), XPA (Abcam) and p62 (3C9, kindly provided by J.M. Egly (Institut de Génétique et de Biologie Moléculaire et Cellulaire)). The polyclonal antibodies used were to Flag (F7425, Sigma), ubiquitin (Z0458, Dako), RNA Pol II (Ab5095, Abcam), Myc (9E10, sc-40, Santa Cruz Biotechnology), USP7 (A300-033A, Bethyl), ERCC6 (E-18, sc-10459, Santa Cruz Biotechnology), p89/XPB (S-19, sc-293, Santa Cruz Biotechnology), HMGN1 (Ab5212, Abcam), KIAA1530 (UVSSA) (NBP1-32598, Novus, and P-12, sc-138374, Santa Cruz Biotechnology) and XPC. Odyssey-compatible secondary antibodies were from LI-COR, and horseradish peroxidase (HRP)-conjugated secondary antibodies were from Dako (to mouse and goat), Southern Biotech (to rabbit) and Sigma (to IgM).

Isolation of ubiquitinated protein complexes. SILAC-labeled HeLa cells were UV irradiated (16 J/m^2) or mock treated. Label swapping was performed to validate the biological findings, aid contaminant removal and exclude possible SILAC-derived differences. One hour after UV cells were washed twice in ice-cold PBS and harvested by scraping in RIPA buffer (PBS containing 1% NP-40, 0.5% sodium deoxycholate and 0.1% SDS) supplemented with 15 μM MG132 (Biomol), 10 mM N-Ethylmaleimide (Sigma), 20 μM PR-619 (LifeSensors) and Complete protease inhibitor cocktail (Roche). Lysates were centrifuged at 16,000*g* at 4 °C for 15 min. Cleared UV- and mock-treated lysates were combined in a 1:1 ratio based on protein concentrations and added to the anti-ubiquitin resin (100 μl slurry per 5.3 mg of lysate) for 4 h at 4 °C. The anti-ubiquitin resin was prepared by incubating 100 μl of 50% ProtG slurry (Pierce) with 87.5 μg of FK2 antibody (Biomol) for 40 min at room temperature, and four washes were performed with RIPA buffer. Protein complexes were eluted (after four washes with RIPA of lysate-bound resin) in two bead volumes of 4% SDS by shaking for 10 min at 1,000 rpm in an Eppendorf Thermomixer. The eluted sample was concentrated over 30-kDa spin columns (Millipore), supplemented with 2× Laemmli buffer and loaded onto 4–15% SDS-PAGE gradient gels (Jule).

Mass spectrometry. SDS-PAGE gel lanes were cut into 2-mm slices and subjected to in-gel reduction with dithiothreitol, alkylation with iodoacetamide (98%; D4, Cambridge Isotope Laboratories) and digested with trypsin (sequencing grade; Promega), as described previously[40]. Nanoflow liquid chromatography tandem mass spectrometry (LC-MS/MS) was performed on an 1100 series capillary liquid chromatography system (Agilent Technologies) coupled to an LTQ-Orbitrap XL mass spectrometer (Thermo Scientific) operating in positive mode. Peptide mixtures were trapped on a ReproSil C18 reversed phase column (Dr Maisch; 1.5 cm × 100 μm) at a rate if 8 μl/min. Peptides were separated on a ReproSil-C18 reversed-phase column (Dr Maisch; 15 cm × 50 μm) using a linear gradient of 0–80% acetonitrile (in 0.1% formic acid) during 170 min at a rate of 200 nl/min using a splitter. The elution was directly sprayed into the electrospray ionization (ESI) source of the mass spectrometer. Spectra were acquired in continuum mode; fragmentation of the peptides was performed in data-dependent mode.

Raw mass spectrometry data were analyzed with MaxQuant software (version 1.1.1.25)[41]. A false discovery rate of 0.01 for proteins and peptides and a minimum peptide length of 6 amino acids were set. The Andromeda search engine[42] was used to search the tandem mass spectrometry (MS/MS) spectra against the International Protein Index (IPI) human database (release 3.68). A maximum of two missed cleavages and mass tolerance of 0.6 Da was allowed. Further modifications were cysteine carbamidomethylation-2D (fixed), protein methionine oxidation and lysine ubiquitination (variable). MaxQuant automatically quantified SILAC peptides and proteins. From the 2,586 identified proteins in the forward and reverse experiments, we removed 116 known contaminants and reverse hits, 411 proteins that had less than 2 quantitation events, 441 proteins that were only found in the forward or reverse experiment, 71 hits with opposite ratios (>1.25-fold) in the label-swap experiment and 311 proteins with background levels (<1.25-fold) in one of the label-swap experiments. The remaining 1,236 proteins were plotted on the S curve (**Fig. 1a**).

For the identification of UVSSA interactors, the software package Scaffold (version 3_00_03, Proteome Software) was used to validate MS/MS based peptide and protein identifications. Peptide identifications were accepted at >95.0% probability with the Peptide Prophet algorithm[43]. Protein identifications assigned by the Protein Prophet algorithm[38,44] were accepted at >95.0% probability.

Clonogenic survival assay. Cells from indicated cell lines were seeded in triplicate in 6-well plates (400 cells/well) and treated with UV-C or IlludinS[15] (24-h exposure) 1 d after seeding. After 1 week, colonies were fixed and stained in 50% methanol, 7% acetic acid and 0.1% Coomassie blue.

Recovery of RNA synthesis and unscheduled DNA synthesis after UV irradiation. Fluorescence-based RRS and UDS were performed as described[16]. In short, for RRS, the cell lines were UV irradiated with 12 J/m^2 of UV-C. Transcription levels were determined 16 h after UV irradiation by 2 h of incubation with ethynyluridine (EU) incorporation. For UDS, VH10 cells

doi:10.1038/ng.2230

were UV irradiated with 16 J/m^2 of UV-C 48 h after siRNA transfection. UDS was determined by 3 h of incubation with 5-ethynyl,2′-deoxyuridine (EdU) incorporation. RRS and UDS were quantified by determining fluorescence intensities for >200 cells with ImageJ software of images obtained with a Zeiss LSM700. The cells displayed in **Figure 2c** were stained with antibody to GFP (Abcam) after the RRS procedure to visualize GFP signal.

Coimmunoprecipitation. Cells expressing Flag-, Myc-, HA- and/or GFP-tagged proteins were treated 24 h after transfection with the indicated UV-C doses and/or with 50 μM MG132 and lysed in RIPA buffer supplemented with Complete protease inhibitor cocktail (Roche) after 1 h of recovery. Lysates were incubated on ice for 10 min and were centrifuged at 16,000*g* for 15 min at 4 °C. The supernatant was incubated for 4 h at 4 °C with antibody-conjugated agarose beads. Beads were washed four times with RIPA buffer and eluted with one bead volume of 2× Laemmli SDS sample buffer at 95 °C.

***In vivo* cross-linking and ChIP.** The procedure for ChIP has been described previously[26]. Briefly, cells were mock treated or exposed to UV-C light (20 J/m^2) and left to recover for 1 h at 37 °C and then cross-linked *in vivo* by 1% formaldehyde at 4 °C. Cross-linked cells were lysed, and purified chromatin was sheared with the Bioruptor Sonicator (Diagenode) using cycles of 30 s on and 60 s off. ChIP was performed on chromatin fragments of 200–600 bp. Reversal of the cross-linking and elution of the precipitated proteins was performed by extended boiling in Laemmli SDS sample buffer, and eluted proteins were analyzed by protein blotting[26].

Live-cell confocal laser-scanning microscopy and immunofluorescence. Confocal laser-scanning microscopy images were obtained with a Leica SP5 confocal microscope using a 100× quartz objective. Kinetic studies of GFP-tagged UVSSA, ERCC6, DDB2 and XPC accumulation were performed using UV-C (266 nm) laser irradiation, as described previously[22]. FRAP experiments were performed as described previously[45]. All FRAP data (average of >15 cells) were normalized to the average fluorescence before bleaching after removal of the background signal.

Immunofluorescence experiments were executed as described[46], with or without pre-extraction by a 20-s treatment with 0.5% Triton X-100 before fixation. GFP-tagged proteins were visualized by staining with an antibody to GFP.

37. Campeau, E. *et al.* A versatile viral system for expression and depletion of proteins in mammalian cells. *PLoS ONE* **4**, e6529 (2009).
38. Epping, M.T. *et al.* TSPYL5 suppresses p53 levels and function by physical interaction with USP7. *Nat. Cell Biol.* **13**, 102–108 (2011).
39. Sugaya, K., Vigneron, M. & Cook, P.R. Mammalian cell lines expressing functional RNA polymerase II tagged with the green fluorescent protein. *J. Cell Sci.* **113**, 2679–2683 (2000).
40. Wilm, M. *et al.* Femtomole sequencing of proteins from polyacrylamide gels by nano-electrospray mass spectrometry. *Nature* **379**, 466–469 (1996).
41. Cox, J. *et al.* A practical guide to the MaxQuant computational platform for SILAC-based quantitative proteomics. *Nat. Protoc.* **4**, 698–705 (2009).
42. Cox, J. *et al.* Andromeda: a peptide search engine integrated into the MaxQuant environment. *J. Proteome Res.* **10**, 1794–1805 (2011).
43. Keller, A., Nesvizhskii, A.I., Kolker, E. & Aebersold, R. Empirical statistical model to estimate the accuracy of peptide identifications made by MS/MS and database search. *Anal. Chem.* **74**, 5383–5392 (2002).
44. Nesvizhskii, A.I., Keller, A., Kolker, E. & Aebersold, R. A statistical model for identifying proteins by tandem mass spectrometry. *Anal. Chem.* **75**, 4646–4658 (2003).
45. Houtsmuller, A.B. & Vermeulen, W. Macromolecular dynamics in living cell nuclei revealed by fluorescence redistribution after photobleaching. *Histochem. Cell Biol.* **115**, 13–21 (2001).
46. Marteijn, J.A. *et al.* Nucleotide excision repair–induced H2A ubiquitination is dependent on MDC1 and RNF8 and reveals a universal DNA damage response. *J. Cell Biol.* **186**, 835–847 (2009).